

η and η' transition form factors from rational approximants

Rafel Escribano,^{1,*} Pere Masjuan,^{2,†} and Pablo Sanchez-Puertas^{2,‡}

¹*Grup de Física Teòrica (Departament de Física) and Institut de Física d'Altes Energies (IFAE),
Universitat Autònoma de Barcelona, E-08193 Bellaterra (Barcelona), Spain*

²*Institut für Kernphysik, Johannes Gutenberg-Universität, D-55099 Mainz, Germany*

(Dated: April 18, 2022)

The η and η' transition form factors in the space-like region are analyzed at low and intermediate energies in a model-independent way through the use of rational approximants. The slope and curvature parameters of the form factors as well as their values at zero and infinity are extracted from experimental data. The impact of these results on the mixing parameters of the η - η' system and the pseudoscalar-exchange contributions to the hadronic light-by-light scattering part of the anomalous magnetic moment a_μ are also discussed.

PACS numbers: 12.38.-t, 12.38.Lg, 12.39.Fe

Keywords: transition form factors, Padé approximants, η - η' mixing, muon anomalous magnetic moment

I. INTRODUCTION

The pseudoscalar transition form factors (TFF) $\gamma^*\gamma \rightarrow P$, where $P = \pi^0, \eta, \eta'$ or η_c , have acquired a lot of attention recently, both from the experimental and theoretical sides, since the release of the *BABAR* data on the π^0 -TFF in 2009 [1]. The TFF describes the effect of the strong interaction on the $\gamma^*\gamma \rightarrow P$ transition and is represented by a function $F_{P\gamma^*\gamma}(q_1^2, q_2^2)$ of the photon virtualities. Measuring both virtualities from the two-photon-fusion reaction $e^+e^- \rightarrow e^+e^-P$ is still an experimental challenge, so the common practice is to extract the TFF when one of the outgoing leptons is tagged and the other is not, that is, the single-tag method. The tagged lepton emits a highly off-shell photon with the momentum transfer $q_1^2 \equiv -Q^2$ and is detected, while the other, untagged, is scattered at a small angle and its momentum transfer q_2^2 is near zero. The form factor extracted from the single-tag experiment is then a function of one of the virtualities: $F_{P\gamma^*\gamma}(Q^2) \equiv F_{P\gamma^*\gamma}(-Q^2, 0)$.

At low-momentum transfer, the TFF can be described by the expansion

$$F_{P\gamma^*\gamma}(Q^2) = F_{P\gamma\gamma}(0) \left(1 - b_P \frac{Q^2}{m_P^2} + c_P \frac{Q^4}{m_P^4} + \dots \right), \quad (1)$$

where $F_{P\gamma\gamma}(0)$ is the normalization, the parameters b_P and c_P are the slope (related to the mean square radius of the meson by $b_P/m_P^2 = \langle r^2 \rangle/6$) and the curvature, respectively, and m_P is the pseudoscalar meson mass. $F_{P\gamma\gamma}(0)$ can be obtained either from the measured two-photon partial width of the meson P ,

$$|F_{P\gamma\gamma}(0)|^2 = \frac{64\pi}{(4\pi\alpha)^2} \frac{\Gamma(P \rightarrow \gamma\gamma)}{m_P^3}, \quad (2)$$

or, in the case of π^0 , η and η' , from the prediction of the axial anomaly in the chiral and large- N_c limits of QCD. For instance, $F_{\pi^0\gamma\gamma}(0) = 1/(4\pi^2 F_\pi)$, where $F_\pi \simeq 92$ MeV is the pion decay constant. The corresponding predictions for the η and η' are discussed below. Concerning the slope parameter, Chiral Perturbation Theory (ChPT) predicts [2, 3] $b_\eta = 0.51$ and $b_{\eta'} = 1.47$ at $\mu^2 = 0.69$ GeV² and for $\sin\theta_P = -1/3$ [4], being μ the renormalization scale and θ_P the η - η' mixing angle in the octet-singlet basis defined at lowest order. Other theoretical predictions are [4]: $b_\eta = 0.53$ and $b_{\eta'} = 1.33$, from Vector Meson Dominance (VMD); $b_\eta = 0.51$ and $b_{\eta'} = 1.30$, from constituent-quark loops (QL); and $b_\eta = 0.36$ and $b_{\eta'} = 2.11$, from the Brodsky-Lepage (BL) interpolation formula [5]. Experimental determinations of these parameters are usually obtained after a fit to data using a normalized, single-pole term with an associated mass Λ_P , *i.e.*

$$F_{P\gamma^*\gamma}(Q^2) = \frac{F_{P\gamma\gamma}(0)}{1 + Q^2/\Lambda_P^2}. \quad (3)$$

At large-momentum transfer, the TFF can be calculated in the asymptotic $Q^2 \rightarrow \infty$ limit at leading twist as a convolution of a perturbative hard scattering amplitude $T_H(\gamma\gamma^* \rightarrow q\bar{q})$ and a gauge-invariant meson distribution amplitude (DA) which incorporates the nonperturbative dynamics of the QCD bound-state [6].

While the low- and large-momentum transfer regions are in principle well described by ChPT and perturbative QCD (pQCD), respectively, it would be highly desirable to have a model-independent description of the TFFs in the whole energy range. Unfortunately, such a description is still lacking for the η and η' [7–20]. In Ref. [21], it was suggested for the π^0 case that this model-independent description can be achieved using a sequence of rational functions, the Padé Approximants (PAs), to fit the experimental data. In this way, not only the low- and large-momentum transfer predictions of ChPT and pQCD should be reproduced but also a reliable description of the intermediate-energy region would be available. The main advantage of the method of PAs is in

* rescriba@ifae.es

† masjuan@kph.uni-mainz.de

‡ sanchezp@kph.uni-mainz.de

deed to provide the Q^2 dependence of the TFF over the whole space-like region in an easy, systematic and model-independent way [21, 22]. This is relevant, for instance, when extrapolating from the asymptotic Q^2 limit to the charmonium region [23]. We also notice that for the forthcoming KLOE-2 [24] and BES-III [25] TFFs measurements will be helpful to have a more reliable model-independent description of the whole energy range, and particularly at low energies, in order to build up a solid Monte Carlo generator for data analysis and feasibility studies.

The aim of this work is then to extend and further develop the application of PAs, already initiated in Refs. [21, 22], to the analysis of η and η' TFFs taking into account η - η' mixing effects systematically. As shown below, this analysis complements our understanding of the η - η' mixing pattern and, more important, can shed light on their relation to the anomalous magnetic moment of the muon, a_μ , through its hadronic light-by-light scattering contribution (HLBL). Preliminary results were presented in Ref. [26].

The paper is organized as follows. In Section II, we briefly describe the general method for extracting low-energy parameters from the TFFs using rational approximants and then apply this method to the case of η and η' TFFs. In Section III, we discuss the implications of our results for the determination of the η - η' mixing parameters. Finally, in Section IV, we analyze the possible impact of our findings on the HLBL piece of a_μ , with special attention to the η and η' exchange contributions. The conclusions are presented in Section V.

II. η AND η' TRANSITION FORM FACTORS AT LOW AND INTERMEDIATE ENERGIES

In order to extract the low-energy parameters b_P and c_P (slope and curvature, respectively) from the available data, we use the method described in Refs. [21, 22]. This method makes use of Padé Approximants as fitting functions to all the experimental data in the space-like region. PAs are rational functions $P_M^N(Q^2)$ (ratio of a polynomial $T_N(Q^2)$ of order N and a polynomial $R_M(Q^2)$ of order M) constructed in such a way that they have the same Taylor expansion as the function to be approximated up to order $\mathcal{O}(Q^2)^{N+M+1}$ [27]. Since PAs are built in our case from the unknown low-energy parameters (LEPs) of the TFF, once the fit to the experimental data is done, the reexpansion of the PAs yields the desired coefficients. We refer the interested reader to Ref. [21] for details on this technique.

The main feature of this method is the usage of a sequence of PAs. In this way, one can ascribe a systematic error to the result due to the expected convergent behavior of the sequence. Being so, the largest the sequence the smallest the systematic error. In a realistic case, however, the sequence will not be infinite since, at some given order, the additional parameters of the fit-

ted PAs will be statistically compatible with zero. Then, one should stop the sequence at that order. The fact that we fit the data using rational functions with a finite number of coefficients instead of an infinite one, leads to an intrinsic or systematic error on the LEPs predictions. In Refs. [21, 22], this error was carefully studied and provided. In accordance with this, we ascribe a conservative 5.6% and 21% of systematic error for the slope and curvature parameters, respectively, to our final LEPs determinations. Since in practice, our PA sequences are quite short (up to 5-6 elements at most), one needs to consider several kind of sequences with different analytical properties for better strengthen the results. This proceeding avoids problems of over-fitting as well. The choice of which type of PA sequence to be used is largely determined by the analytic properties of the function to be approximated. As argued in Ref. [21], the time-like region for the π^0 -TFF exhibits a predominant role of the ρ meson contribution with the excited states being much suppressed. For the η - and η' -TFF, the appropriate combination of ρ , ω and ϕ should play the same role through an effective single-pole dominance as the ρ on the π^0 -TFF. For that reason, a $P_1^L(Q^2)$ sequence (single-pole approximants) seems the optimal choice in the η and η' . However, according to Ref. [6], the pseudoscalar TFFs behave as $1/Q^2$ for $Q^2 \rightarrow \infty$, which means that, for any value of L , one will obtain in principle a good fit only up to a finite value of Q^2 but not for $Q^2 \rightarrow \infty$. Therefore, it would be desirable to incorporate this asymptotic limit information in the fits by considering also a $P_N^N(Q^2)$ sequence.

In the following subsection, we present and discuss the obtained weighted averaged results for the slope and curvature parameters of the η - and η' - TFFs from all the PA sequences mentioned above. We remark that since it is common to publish experimental data on $Q^2 F_{\eta^{(\prime)}\gamma^*\gamma}(Q^2)$ instead of $F_{\eta^{(\prime)}\gamma^*\gamma}(Q^2)$, we fit directly the former. We do that in a bottom-up approach to warrant any prejudice against the results. We should start fitting $Q^2 F_{\eta^{(\prime)}\gamma^*\gamma}(Q^2)$ space-like data, without using any information about $Q^2 = 0$. That means, in particular, that $\lim_{Q^2 \rightarrow 0} Q^2 F_{\eta^{(\prime)}\gamma^*\gamma}(Q^2) = 0$ is not imposed but extracted from data. A second step should incorporate such information by, for example, making use of PAs that its numerator starts already at order Q^2 (i.e., $T_N(0) = 0$). That should allow us to predict the value of the two-photon partial width from pure space-like data, on top of the slope and curvature of the TFF. Finally, as a last step, we should incorporate that two-photon partial width in our set of data to be fitted together with the space-like data. This bottom-up approach should allow us to strengthen systematically our results.

A. η and η' Transition Form Factors

For both the η and η' TFFs, we collect the experimental information from the CELLO, CLEO, *BABAR*

and L3 Collaborations [28–31]. For our bottom-up approach we include in our final step the values $\Gamma_{\eta \rightarrow \gamma\gamma} = 516(18)$ eV (obtained after combining the current PDG average [32] together with the recent KLOE-2 Collaboration [33] result) and $\Gamma_{\eta' \rightarrow \gamma\gamma} = 4.34(14)$ keV from the PDG [32]. Since the asymptotic values of the space-like and time-like TFFs are expected to be very similar, we also comment on the results when including in our analysis the time-like measurements¹ for the η and η' reported by the *BABAR* Collaboration [34].

We start our bottom-up approach by fitting space-like data without including the constraint that the $\lim_{Q^2 \rightarrow 0} Q^2 F_{\eta^{(\prime)}\gamma^*\gamma}(Q^2) = 0$. This first step yields rather bad fits although we notice that for the η case, our fit “sees the zero” at less than three standard deviations (fitting with a $P_1^1(Q^2)$, the first coefficient t_0 , which is expected to be 0, is found to be $t_0 = 0.061(26)$). For the η' case, the results are much better, and the zero is seen by less than one sigma. Indeed, we reach a $P_1^3(Q^2)$ and found $t_0 = -0.001(3)$. In this case, we can also look for the next coefficient. We find $t_1 = 0.35(5)$ GeV⁻¹ which, making use of Eq. (2), predicts $\Gamma_{\eta' \rightarrow \gamma\gamma} = 4.5(1.3)$ keV. This fact illustrates the potentiality of the space-like data, which ranges from 0.6 GeV² to 35 GeV² for the η and from 0.06 GeV² to 35 GeV² for the η' , to shed light on the low-energy region.

Including in the following the $\lim_{Q^2 \rightarrow 0} Q^2 F_{\eta^{(\prime)}\gamma^*\gamma}(Q^2) = 0$, i.e., making use of PAs which numerator starts already at order Q^2 , the fits with our best approximants are shown in Fig. 1 for η - and η' -TFF respectively from both scenarios: *without* and *with* the two-photon partial width included in the data set. Its LEPs are collected in Table I and Table II and shown in Figs. 2 and 3. The stability of our low-energy parameters with the $P_1^L(Q^2)$ is quite reassuring. We include in these figures 2 and 3 the results obtained by the CELLO Collaboration [28] using a Vector Meson Dominance model fit. The curvature is obtained by expanding the VMD used in [28]. We add to their determination the same systematic error as we include in our determinations, which turns out to be 44% following Refs. [21, 22].

In Appendix A we provide our best fit parameterizations for both η - and η' -TFFs when the constrain at $Q^2 = 0$ and the $\Gamma_{P \rightarrow \gamma\gamma}$ are included, that can be used, for example, to predict the time-like TFF. Applying such parameterization for the $\eta \rightarrow e^+e^-\gamma$ Dalitz decay, we find a perfect agreement with experimental data [35].

All the different approximants considered lead to compatible results, although including the two-photon par-

tial width is crucial in the LEPs predictions for two reasons: the first one is that smaller error on such decays immediately yields smaller error on slope and curvature; the second one, and more important, is that precise two-photon partial width allow us to reach higher approximants in our sequences, rendering smaller systematic errors. Precise measurements of such partial widths will be very welcome, then, to better extract, from statistics and systematics, the low-energy parameters. Notice, however, that the two-photon partial width is well determined by our fits. Using Eq. (2) and the predictions for $F_{\eta^{(\prime)}\gamma^*\gamma}(0)$ from Table I, we predict such partial width to be $\Gamma_{\eta \rightarrow \gamma\gamma} = 0.41(18)$ KeV and $\Gamma_{\eta' \rightarrow \gamma\gamma} = 4.21(43)$ KeV. These results only differ to the measured ones by 0.6 and 0.3 standard deviations respectively. We remark the role of the high-energy TFF data to obtain large PA sequence which allow good determinations of the LEPs. Precise experimental data on the high-energy region is, then, also important for the low-energy region.

The last raw in Tables I and II show our final result obtained after a weighted average of the different determinations. The main results of this work are shown in Table II while the results in Table I are kept for comparison on the stability of our fits.

In the following we comment only about the results in Table II.

For η and η' , the $P_1^L(Q^2)$ sequences reaches $L = 5$ and $L = 6$ respectively as the best approximant. The fitted poles $\sqrt{s_p}$ of these sequences range $\sqrt{s_p} = (0.72 - 0.77)$ GeV and $\sqrt{s_p} = (0.80 - 0.86)$ GeV for η and η' respectively, as can be seen in Fig. 4. For comparison we also show as orange and blue bands (corresponding to the η and the η' case respectively) what would correspond to the effective VMD meson resonance m_{eff} for each case [37]. The band represents the range of such mass value due to the half width rule [38–40], i.e., $m_{eff} \pm \Gamma_{eff}/2$. For the η we obtain $m_{eff} = 0.732(72)$ GeV and for the η' $m_{eff} = 0.822(58)$ GeV with errors coming from the half-width rule [38–40]. Raising the pole lowers $b_{\eta,\eta'}$ and $c_{\eta,\eta'}$ values and vice-versa. Fitting space-like data does not produce an accurate determination of the resonance poles as already indicated in Refs. [21, 22, 41, 42]. We advice not to use this method for such determination. That include the usage of VMD fits to determine such resonance parameters. An alternative model-independent procedure to extract these parameters using PAs can be found in Ref. [43].

To reproduce and estimate the asymptotic limit for the TFF, we should consider the $P_N^N(Q^2)$ (second row in Table II, with results in nice agreement with the previous determinations). Our best fit is shown as a black-solid line in Fig. 1. We reach $N = 2$ for the η -TFF and $N = 1$ for the η' -TFF. Since these approximants contain the correct high-energy behavior built in, they can be extrapolated to infinity (black-dashed lines in Fig. 1), and one can try to predict the leading $1/Q^2$ coefficient:

¹ The time-like TFF for the π^0 at high energy is not yet available, but it could be measured at $q^2 = 14.6$ GeV² by the BES-III Collaboration [25]. This particular point is in the region, reaching the asymptotic limit, where the measurements from the *BABAR* and Belle Collaborations start to differ, so we encourage BES-III to measure it.

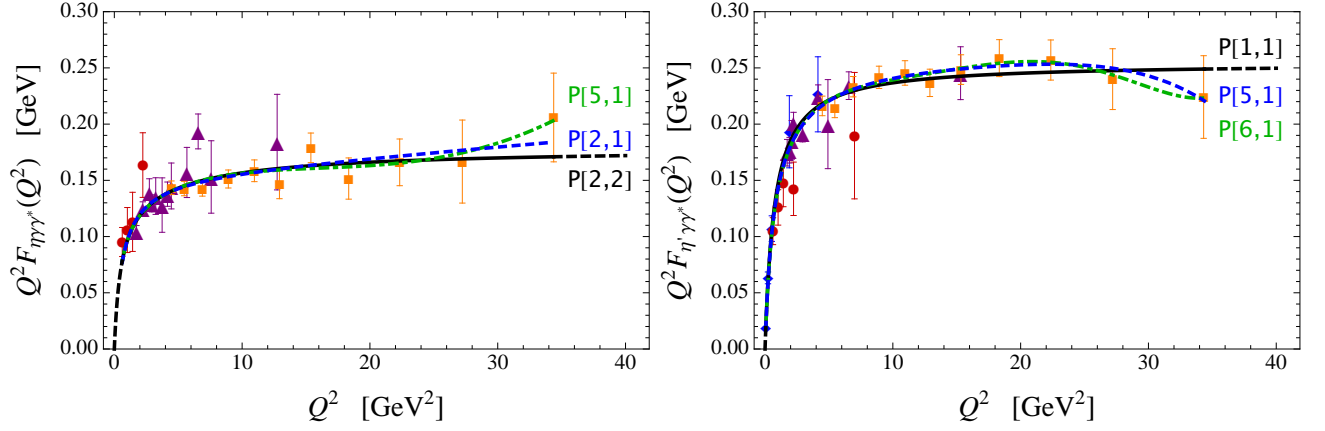


FIG. 1. η - and η' -TFFs best fits (left and right panels reps.). Blue dashed line shows our best $P_1^L(Q^2)$ when the two-photon partial decay width is *not* included in our set of data to be fitted. When the two-photon partial decay width *is* included, dark-green dot-dashed line shows our best $P_1^L(Q^2)$, and black solid line shows our best $P_N^N(Q^2)$. Black dashed lines are the extrapolation of such approximant at $Q^2 = 0$ and at $Q^2 \rightarrow \infty$. Data points are from CELLO (red circles) [28], CLEO (purple triangles) [36], L3 (blue diamonds) [31], and *BABAR* (orange squares) [30] Collaborations. See main text for details.

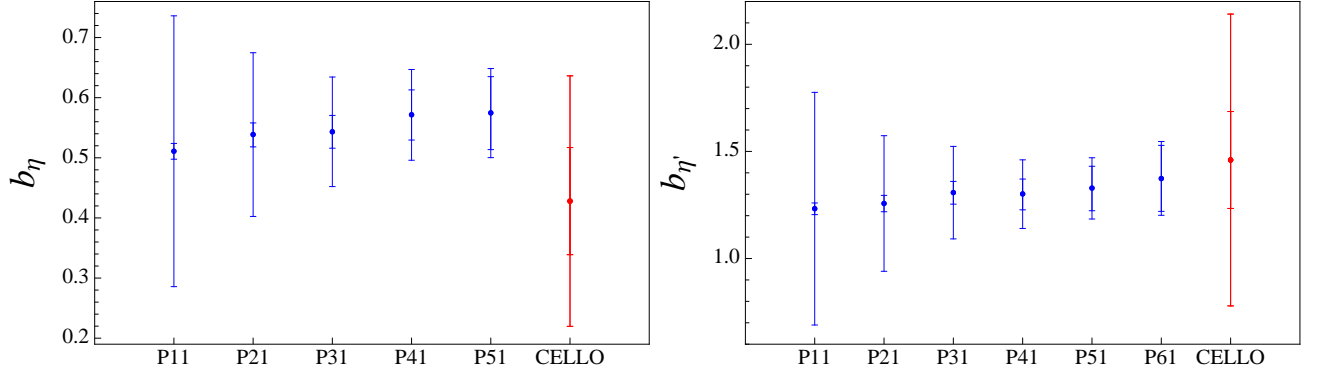


FIG. 2. Slope predictions with the $P_1^L(Q^2)$ up to $L = 5$ and $L = 6$ for the η -TFF and the η' -TFF (left and right panels respectively). The internal band is the statistical error from the fit and the external one is the combination of statistical and systematic errors determined in the previous section.

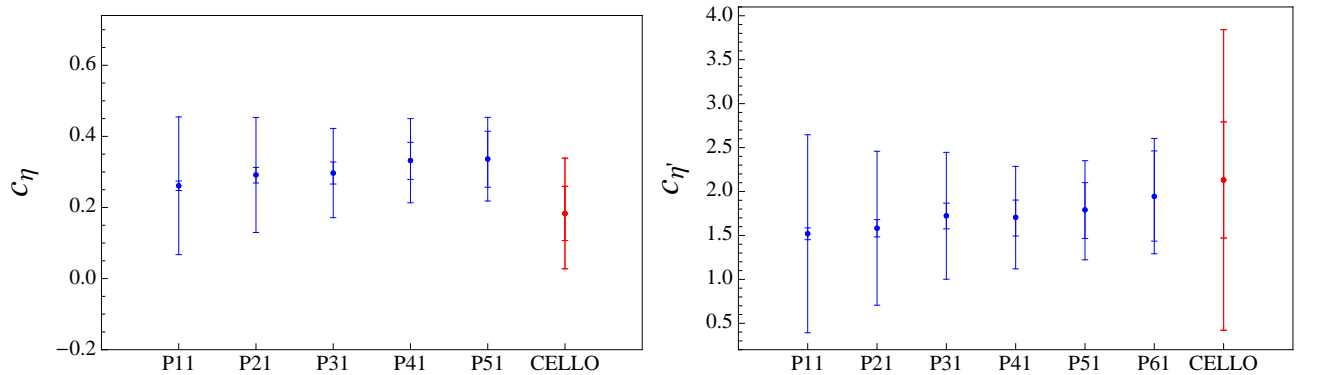


FIG. 3. Curvature predictions with the $P_1^L(Q^2)$ up to $L = 5$ and $L = 6$ for the η -TFF and the η' -TFF (left and right panels respectively). The internal band is the statistical error from the fit and the external one is the combination of statistical and systematic errors determined in the previous section.

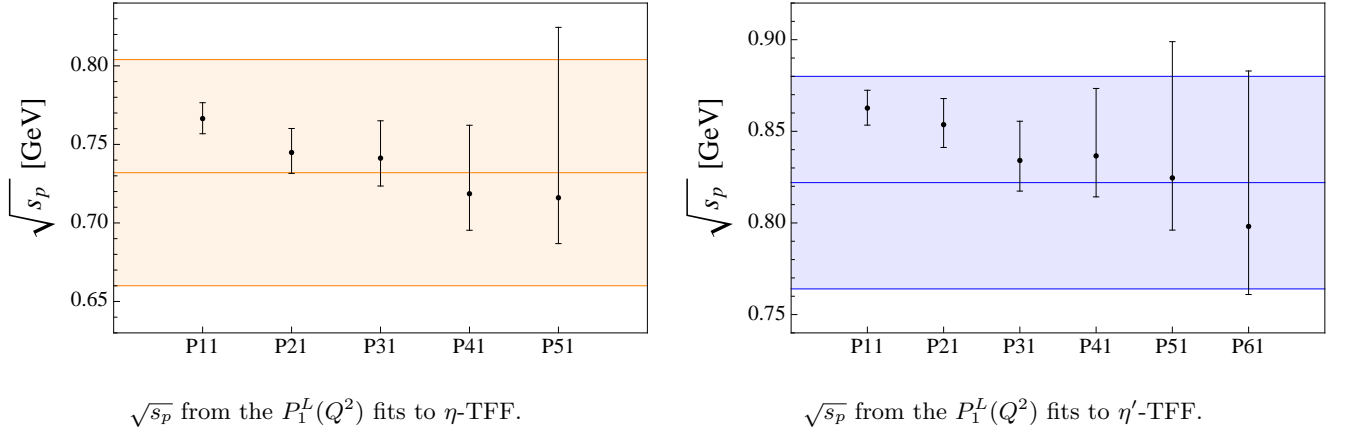


FIG. 4. Pole position $\sqrt{s_p}$ for the different $P_1^L(Q^2)$ after the fits to the η - and η' -TFF, resp. For comparison we also show (orange and blue bands) the range $M_{eff} \pm \Gamma_{eff}/2$ corresponding to the VMD effective-meson value ranged by its half-width (see main text for details).

$$\begin{aligned} \lim_{Q^2 \rightarrow \infty} Q^2 F_{\eta\gamma^*\gamma}(Q^2) &= 0.164(21) \text{ GeV}, \\ \lim_{Q^2 \rightarrow \infty} Q^2 F_{\eta'\gamma^*\gamma}(Q^2) &= 0.254(4) \text{ GeV}. \end{aligned} \quad (4)$$

We remark that the inclusion of the two-photon partial decay width in the η -TFF case allowed us to reach $N = 2$ and reduce the uncertainty drastically. Otherwise, we would have remained at $N = 1$ with errors five times larger.

Finally, our combined weighted average result from Table II leads to

$$\begin{cases} b_\eta = 0.596(48)_{stat}(33)_{sys} \\ c_\eta = 0.362(66)_{stat}(76)_{sys} \times 10^{-3} \\ b_{\eta'} = 1.37(16)_{stat}(8)_{sys} \\ c_{\eta'} = 1.94(52)_{stat}(41)_{sys} \times 10^{-3} \end{cases} \quad (5)$$

where the second error is the systematic one (5.6% and 21% for b_P and c_P respectively). The η results are the result of averaging the $P_1^5(Q^2)$ and the $P_2^2(Q^2)$. The latter has smaller systematic error of about 3% but we keep the one for $P_1^5(Q^2)$ since is the largest. Eq. (5) represent one of the main results of this work.

When the spread of central values considered for the weighted averaged result is larger than the error after averaging, we enlarge it to cover such spread². For the fits to η' with the $P_N^N(Q^2)$ sequence we could only reach $N = 1$ which turns out to be the first element on the $P_1^L(Q^2)$ sequence. The first element of each sequence is the worse one and then should not be used for our final averaged results.

In Ref. [30], *BABAR* Collaboration provide with a measurement of the time-like TFF for both η and η' at $Q^2 = (10.58)^2 \text{ GeV}^2$. Including these determinations into our set of data does not modify our LEPs predictions at the precision we are reporting them in this work.

The b_η slope may be compared with $b_\eta = 0.428(89)$ from CELLO [28] and $b_\eta = 0.501(38)$ from CLEO [29], and $b_\eta = 0.51$ from ChPT [4]. The TFF was also measured in the time-like region reporting $b_\eta = 0.57(12)$ by the Lepton-G [44], $b_\eta = 0.585(51)$ by NA60 [45], $b_\eta = 0.58(11)$ by MAMI [35], and $b_\eta = 0.68(26)$ by WASA [46]. One should notice that all the previous collaborations used a VMD model fit to extract the slope. In order to be consistent when comparing with our result, a systematic error about 44% should be added to these results [21].

The $b_{\eta'}$ slope can be compared with $b_{\eta'} = 1.46(23)$ from CELLO [28] and $b_{\eta'} = 1.24(8)$ from CLEO [29], and also with $b_{\eta'} = 1.47$ using ChPT [4]. From the time-like analysis done by Lepton-G Collaboration (cited in [37]) $b_{\eta'} = 1.6(4)$. Again, a 44% of systematic error should be added to these experimental extractions done with a VMD fit.

The quality of our fits is accounted for the χ^2/dof (dof defined as degrees of freedom) and collected in the last column of both Table I and II. We remark that the χ^2/dof are slightly smaller than 1 as a sign of a missing theoretical error on our analysis. We amend that with the inclusion of the systematic error.

Finally, we want to comment on the effective single-pole mass determination $b_P = m_P^2/\Lambda_P^2$ from Eq. (3). Using the values in Eq. (5), we obtain $\Lambda_\eta = 0.710 \text{ GeV}$ and $\Lambda_{\eta'} = 0.818 \text{ GeV}$. These numbers together with $\Lambda_\pi = 0.750 \text{ GeV}$ obtained in Ref. [21] implies $\Lambda_\eta < \Lambda_\pi < \Lambda_{\eta'}$, in agreement with quark loop and VMD model computations [4].

² We thank C.F. Redmer for discussions on the average procedure.

TABLE I. Low-energy parameters for the η - and η' -Transition Form Factor obtained from the PA fits to experimental data *without* including the two-photon partial decay width in the set of data to be fitted. The first column indicates the kind of sequence used for the fit and N is the highest order reached with that sequence. The final row gives the weighted average result for each LEP. We also give the quality of the fits represented by the χ^2/dof (degree of freedom). Errors are symmetrized.

	ηTFF					$\eta' TFF$				
	N	b_η	c_η	$F_{\eta\gamma\gamma}(0)\text{GeV}^{-1}$	χ^2/dof	N	$b_{\eta'}$	$c_{\eta'}$	$F_{\eta'\gamma\gamma}(0)\text{GeV}^{-1}$	χ^2/dof
$P[N, 1]$	2	0.47(14)	0.22(13)	0.244(55)	0.82	5	1.23(16)	1.69(42)	0.338(17)	0.79
$P[N, N]$	1	0.37(6)	0.13(1)	0.205(28)	0.84	1	1.18(7)	1.38(15)	0.328(14)	0.77
Final		0.47(14)	0.22(13)	0.244(55)			1.23(16)	1.69(42)	0.338(17)	

TABLE II. Low-energy parameters for the η - and η' -Transition Form Factor obtained from the PA fits to experimental data *including* the two-photon partial decay width in our dataset. The first column indicates the kind of sequence used for the fit and N is the highest order reached with that sequence. The final row gives the weighted averaged result for each LEP. We also give the quality of the fits represented by the χ^2/dof (degree of freedom).

	ηTFF				$\eta' TFF$			
	N	b_η	c_η	χ^2/dof	N	$b_{\eta'}$	$c_{\eta'}$	χ^2/dof
$P[N, 1]$	5	0.575(61)	0.336(79)	0.85	6	1.37(16)	1.94(52)	0.78
$P[N, N]$	2	0.63(9)	0.42(12)	0.82	1	1.23(3)	1.52(7)	0.77
Final		0.596(48)	0.362(66)			1.37(16)	1.94(52)	

III. $\eta - \eta'$ MIXING FROM THE TFFS

In Section II A the η - and η' -TFF were analyzed with the $P_N^N(Q^2)$ in order to predict the leading $1/Q^2$ coefficient. With this information at hand together with the predicted values of the $F_{\eta(\prime)\gamma\gamma}(0)$, one can consider to explore the $\eta - \eta'$ mixing in the flavor basis³ [48–60].

In this base, the η and η' decay constants are:

$$\begin{pmatrix} f_\eta^q & f_\eta^s \\ f_{\eta'}^q & f_{\eta'}^s \end{pmatrix} = \begin{pmatrix} f_q \cos \phi_q & -f_s \sin \phi_s \\ f_q \sin \phi_s & f_s \cos \phi_s \end{pmatrix}, \quad (6)$$

where $f_{q,s}$ are the light-quark (strange) decay constants for the corresponding light- and strange-quark content of the η and η' , and ϕ_q and ϕ_s its corresponding mixing angles. The asymptotic limits take then the form:

$$\begin{aligned} \lim_{Q^2 \rightarrow \infty} Q^2 F_{\eta\gamma\gamma^*}(Q^2) &= f_\eta^q \frac{10}{3} + f_\eta^s \frac{2\sqrt{2}}{3}, \\ \lim_{Q^2 \rightarrow \infty} Q^2 F_{\eta'\gamma\gamma^*}(Q^2) &= f_{\eta'}^q \frac{10}{3} + f_{\eta'}^s \frac{2\sqrt{2}}{3}. \end{aligned} \quad (7)$$

Using Eq. (7) and the two equations for the two-photon partial decay width in such base:

³ For an extended and more detailed discussion together with the role of the gluonium on the flavor mixing scheme, see Ref. [47].

$$\begin{aligned} \Gamma_{\eta\gamma\gamma} &= \frac{\alpha^2}{32\pi^3} m_\eta^3 \left(\frac{f_{\eta'}^s \left(\frac{5}{3\sqrt{2}} \right) - f_{\eta'}^q \left(\frac{1}{3} \right)}{f_{\eta'}^s f_\eta^q - f_{\eta'}^q f_\eta^s} \right)^2, \\ \Gamma_{\eta'\gamma\gamma} &= \frac{\alpha^2}{32\pi^3} m_{\eta'}^3 \left(\frac{f_\eta^s \left(\frac{5}{3\sqrt{2}} \right) - f_\eta^q \left(\frac{1}{3} \right)}{f_\eta^s f_{\eta'}^q - f_\eta^q f_{\eta'}^s} \right)^2, \end{aligned} \quad (8)$$

we can attempt to predict such mixing parameters with the results obtained with our fits.

Different phenomenological and theoretical calculations [48–60] provide with different values for those parameters. In the flavor basis, those studies agree on the assumption $\phi_q = \phi_s = \phi$, which means that only three parameters are needed to constrain the mixing, f_s, f_q and ϕ .

We notice that the asymptotic limit for the η' -TFF is well determined for both scenarios (including and not including the two-photon partial width into the fits) with our $P_N^N(Q^2)$ fits to be $\lim_{Q^2 \rightarrow \infty} Q^2 F_{\eta'\gamma\gamma^*}(Q^2) = 0.254(4)$ GeV, and $\lim_{Q^2 \rightarrow \infty} Q^2 F_{\eta\gamma\gamma^*}(Q^2) = 0.256(4)$ GeV respectively, in good agreement with the BABAR time-like measurement at 112 GeV². For both cases, we reach $N = 1$.

For the η -TFF we found, for the first scenario (*without* including the two-photon partial width) $\lim_{Q^2 \rightarrow \infty} Q^2 F_{\eta\gamma\gamma^*}(Q^2) = 0.168(6)$ GeV with our $P_1^1(Q^2)$. *Including* the partial width, we found $\lim_{Q^2 \rightarrow \infty} Q^2 F_{\eta\gamma\gamma^*}(Q^2) = 0.164(21)$ GeV with our $P_2^2(Q^2)$. Both results agree well with the phenomeno-

logical/theoretical range (0.13 – 0.19) GeV [48–60].

These two asymptotic-limit constraints together with the fitted values for the decay widths $\Gamma_{\eta \rightarrow \gamma\gamma} = 516(18)$ eV, and $\Gamma_{\eta' \rightarrow \gamma\gamma} = 4.34(14)$ keV (very similar to the experimental ones), allow us to fix the three parameters of the mixing in three different ways since we have four equations to determine three unknowns. When predicting the asymptotic limit of the η' -TFF with the $P_N^N(Q^2)$ sequence, we could reach the $N = 1$ element only and no further checks of stability of such prediction could be produced. The first element of each PA sequence has the smallest statistical error in its parameters (since that element has the smallest set of parameters to be fitted) but the largest systematic error. On the contrary, for the η -TFF, we could reach $N = 2$ and we indeed see such stabilization. We should not use the η' -TFF determination when exploring the mixing. We expect better results for such parameter when more precise information of the low-energy region for the TFF would be available. In all our numerical computations we use $f_\pi = 0.0922$ GeV, $m_\eta = 547.862$ MeV, and $m_{\eta'} = 957.78$ MeV [32].

As we did in the previous subsection, we report the results for the mixing parameters considering both scenarios, including or not including the two-photon partial width in our fits. The error on the results include the systematic error from our fit procedure. For the asymptotic determination we ascribe a 1% error for the $P_2^2(Q^2)$.

In the first scenario (i.e., *without* that partial width), using the asymptotic value prediction for the η -TFF (obtained with a $P_1^1(Q^2)$) together with the two predicted partial decay widths, we obtain:

$$f_q = 1.21(7) \text{ GeV}, \quad f_s = 1.5(2) \text{ GeV}, \quad \phi = 45(3)^\circ \quad (9)$$

In the second scenario (i.e., *with* the partial width included in the fits), the mixing parameters are predicted to be

$$f_q = 1.07(1) \text{ GeV}, \quad f_s = 1.53(23) \text{ GeV}, \quad \phi = 40.2(1.6)^\circ \quad (10)$$

Eq. (10) represents our final result for the mixing parameters in the flavor basis. This result can be compared, for example, with the update determination of such mixing parameters obtained in Ref. [56] including the up-to-date experimental determinations collected in the last edition of the Particle Data Tables [32]. That reference used a fit to 9 different observables (6 decays $V \rightarrow P\gamma$ with $V = \rho, \omega, \phi$ and $P = \eta, \eta'$ together with the ratio $J\Psi \rightarrow \eta\gamma/J\Psi \rightarrow \eta'\gamma$ and the two-photon partial decay widths for η and η') to obtain the mixing parameters. Using the last PDG collection [32], we update the results in Ref. [56]:

$$f_q = 1.07(1)\text{GeV}, \quad f_s = 1.63(3)\text{GeV}, \quad \phi = 39.6(0.4)^\circ. \quad (11)$$

The agreement between both determinations (10) and (11) is quite astonishing since we only use the information of the TFF to predict the mixing parameters. We notice, however, that using the asymptotic value of the η' -TFF instead of the η counterpart, we obtain much worse results:

$$f_q = 1.01(2) \text{ GeV}, \quad f_s = 0.95(4) \text{ GeV}, \quad \phi = 33.2(0.7)^\circ. \quad (12)$$

The discrepancy between results might be an indication of the lack of stability of the $P_1^1(Q^2)$ to predict the asymptotic limit along the lines commented above or the fact that the η - η' mixing scheme used here is not complete enough to catch the physical features of the mixing (higher order effects on the chiral and large- N_c expansions or including gluonium effects could be of certain importance). Further investigations are relegated to another publication [47]. Precise determinations of the mixing parameters in the flavor basis obtained with the Lattice QCD techniques will be very welcome, also for the implications of such mixing into the light-by-light scattering contribution on the anomalous magnetic moment of the muon, which will be the subject of the next section.

IV. IMPLICATIONS ON THE HADRONIC LIGHT-BY-LIGHT CONTRIBUTION TO THE $(g - 2)_\mu$

The hadronic contributions to the anomalous magnetic moment of the muon a_μ consists on hadronic vacuum polarization as well as hadronic light-by-light scattering (HLBL). The latter cannot be directly related to any measurable cross section and requires the knowledge of QCD contributions at all energy scales. Since this is not known yet, one relies on hadronic models to compute it [61–75]. Indeed, the theoretical value of a_μ is currently limited by uncertainties from the HLBL scattering contribution leading to an uncertainty in a_μ of $(2.6 - 4) \times 10^{-10}$ [76–78] as well as the one from hadronic vacuum polarization $(4.2 - 4.9) \times 10^{-10}$ [79, 80].

The present world average experimental value is given by $a_\mu^{EXP} = 11659208.9(6.3) \times 10^{-10}$ [81, 82], still limited by statistical errors, and a proposal to measure the muon $(g - 2)_\mu$ to a precision of 1.6×10^{-10} has recently been submitted to FNAL [83]. In view of this proposal, it is important to have better control on the HLBL contribution which as we will see may demand also better control on the TFF studied so far.

A complete discussion of HLBL contributions involves the full rank-four hadronic vacuum polarization $\Pi_{\mu\nu\lambda\rho}(q_1, q_2, q_3)$. However, using the large- N_c limit of QCD [84, 85] and also the chiral counting, it was proposed in [86] to split the HLBL into a set of different contributions where the numerically dominant one arises from the pseudo-scalar exchange piece (see Ref. [77] for details). Indeed, it was shown in [65] that this piece

accounts $a_\mu^{HLBL;\pi^0} \sim 7 \times 10^{-10}$, followed by the η and η' contributions ($a_\mu^{HLBL;\eta^{(\prime)}} \sim 1.5 \times 10^{-10}$). The main ingredient on the determination of the pseudoscalar-exchange process $a_\mu^{HLBL,PS}$ is the double off-shell TFF $F_{P^*\gamma^*\gamma^*}((q_1+q_2)^2, q_1^2, q_2^2)$ with a dominant piece when the pseudoscalar is on-shell [65]. The TFF should be considered to be off-shell (see Refs. [67, 68, 71, 77, 78] where this point is addressed). Since such effects for the η and η' are not known, we should keep the pseudoscalar-pole simplifications in our calculations.

In this section we plan to study the impact of the results obtained in the Section II to the HLBL with the intuition that it is more important to have a good description at small and intermediate energies, e.g., by reproducing the slope and curvature of the TFFs, than a detailed short-distance analysis since the angular integrals used to compute a_μ^{HLBL} do not seem to be very sensitive to the correct asymptotic behavior for large momenta [65]. With our model-independent results for the LEPs on the TFF collected in Table II we expect to have a reliable account for the pseudoscalar contribution to a_μ^{HLBL} . For completeness, we also collect the results for the π -TFF obtained in Ref. [74] (i.e. $a_\mu^{HLBL,\pi^0} = 6.49(56) \cdot 10^{-10}$ and $a_\mu^{HLBL,\pi^0} = 6.51(71) \cdot 10^{-10}$ for the first and second elements on the PA sequence, with the full offshell TFF obtained with the same method used in this work) in order to provide $a_\mu^{HLBL,PS}$, i.e., the pseudoscalar exchange contributions to the hadronic light-by-light scattering part of the anomalous magnetic moment a_μ .

In the Large- N_c limit, QCD Green's functions consist of infinitely many non-interacting sharp mesons states whose masses and decay constants are in principle unknown. As such sum is not known in practice, one ends up truncating the spectral function in a resonance saturation scheme, the so-called Minimal Hadronic Approximation [87]. The resonance masses used in each calculation are then taken as the physical ones from PDG instead of the corresponding masses in the large- N_c limit. The effect of the spectrum truncation should be taken into account on the final systematic error [41, 88].

A way of evade these caveats comes from the Padé Theory [41]. In this context, there are two similar approaches that can be considered to compute $a_\mu^{HLBL,PS}$. The first one follows closely the one suggested in Ref. [74], which defines the TFF as a PA built from its LEPs:

$$F_{P^*\gamma^*\gamma^*}^{P01}(Q_1^2, Q_2^2) = P_1^0(Q_1^2, Q_2^2) = a \frac{b}{Q_1^2 + b} \frac{b}{Q_2^2 + b}, \quad (13)$$

where the free parameters are matched at low energies with the results in Table I: a is fixed by $\Gamma_{P \rightarrow \gamma\gamma}$ and b by a matching to the slope b_P .

The convergence of the PA sequence to a meromorphic function is guaranteed by Pomerence's theorem [89]. The problem is to know how fast this convergence is and also how to ascribe a systematic error on each element of that sequence. For the particular case of a meromorphic func-

tion (such as a Green's function in large- N_c QCD), the simplest way of evaluating a systematic error is by comparing the difference between two consecutive elements on the PA sequence [90] (see Appendix B for details).

In our approach to the TFF, we evaluate the systematic error by computing a second element on the PA sequence and compare it with the result using Eq. (13). The second element is:

$$\begin{aligned} F_{P^*\gamma^*\gamma^*}^{P12}(Q_1^2, Q_2^2) &= \\ &= P_2^1(Q_1^2, Q_2^2) = \frac{a + b Q_1^2}{(Q_1^2 + c)(Q_1^2 + d)} \frac{a + b Q_2^2}{(Q_2^2 + c)(Q_2^2 + d)}, \end{aligned} \quad (14)$$

with four coefficients to be matched with $\Gamma_{P \rightarrow \gamma\gamma}$, the slope b_P , the curvature of the TFF c_P and the first effective vector meson resonance accounted for the appropriate ρ, ω, ϕ mixing [37], illustrated in Fig. 4. The error for the effective mass is taken from the half-width rule [38, 39]. The results are collected in Table III. The weighted average results for the low-energy parameters of the η' -TFF collected in Table II considered only the $P_1^L(Q^2)$ sequence since the $P_N^N(Q^2)$ only reached the first element on that sequence. Therefore, in the determination of the $a_\mu^{HLBL;\eta'}$ in Eq. (14) we used the low-energy parameter of order $\mathcal{O}(Q^2)^3$ instead of the effective mass obtained in Ref. [37]. Both procedures yield similar results.

The similarity of the results obtained within both approximants (13) and (14) indicates, as expected [75], that the low-energy region (up to 1 – 2 GeV) dominates the contribution to a_μ^{HLBL} . To evaluate the error on our approximation we look for the maximum of the difference in the region up to 1 GeV between the $P_1^0(Q_1^2, Q_2^2)$ and $P_2^1(Q_1^2, Q_2^2)$ as explained in Ref. [90]. Of course, this difference depends on the energy, and grows as the energy increases. At 1 GeV, the relative difference is about 5% (see Appendix B for details on this estimation), and we take this error as a conservative estimate of the error on the whole low-energy region. We should add this error to the $a_\mu^{HLBL,PS}$ final result. In Appendix B we try another more rigorous way of estimating such error. Since the result there gives smaller error, we keep the 5%.

There is a second way of computing the HLBL that would reassess our previous results. This approach takes into account that the machinery to compute the HLBL used here and given in Ref. [65] belongs to the large- N_c . A way to incorporate in such choice the next-to-leading $1/N_c$ effects is to make use of meson dominance and the half-width rule when accounting for the TFF (see Refs. [38, 39, 91]). Meson dominance means to take the high-energy behavior given by pQCD and the minimal number of mesons to satisfy these conditions. Then, errors in the meson-dominated form factors are estimated by the half-width rule, i.e., by treating resonance masses as random variables distributed with the dispersion given by the width. In this way,

$F_{P\gamma\gamma^*}(Q_1^2, Q_2^2)$	η	η'	Total
$P_1^0(Q_1^2, Q_2^2)$	1.27(16)	1.15(13)	8.91(60)
$P_2^1(Q_1^2, Q_2^2)$	1.27(17)	1.15(11)	8.93(74)
Eq. (15)	1.35(25)	1.16(16)	8.22(76)
Eq. (16)	1.16(21)	1.61(47)	8.53(64)

TABLE III. Collection of results for the $a_\mu^{HLBL;PS}$ for $PS = \eta$ and η' contributions. The last column contains also the result obtained in Ref. [74] for the π^0 -TFF, with errors combined in quadrature. Results in units of 10^{-10} .

$$F_{P\gamma^*\gamma}(Q^2) = \frac{1}{4\pi^2 f_P} \frac{m_{eff}^2}{m_{eff}^2 + Q^2}, \quad (15)$$

provided one has the relation $m_{eff}^2 = 8\pi^2 f_P^2$ to satisfy the asymptotic limit. m_{eff} corresponds to the VMD for each π^0, η, η' TFF [37]. We remind the reader that for the η we obtain $m_{eff} = 0.732(72)$ GeV and for the η' $m_{eff} = 0.822(58)$ GeV. The errors come from the half-width rule. For the π^0 case, $m_{eff} = m_\rho$. If we include two resonances, m_{eff} and $m_{eff'}$, we get, after imposing the anomaly and large- Q^2 behavior,

$$F_{P\gamma^*\gamma}(Q^2) = \frac{1}{4\pi^2 f_P} \frac{m_{eff}^2 m_{eff'}^2 + 8f_P^2 \pi^2 Q^2}{(m_{eff}^2 + Q^2)(m_{eff'}^2 + Q^2)}. \quad (16)$$

The results using both Eqs. (15) and (16) are shown in Table III. For the π^0 case, using $m_\rho = 0.775$ GeV, $m_{\rho'} = 1.465$ GeV, $\Gamma_\rho = 0.150$ GeV and $\Gamma_{\rho'} = 0.400$ GeV, we obtain $a_\mu^{HLBL;\pi^0} = 5.72(70) \cdot 10^{-10}$ and $a_\mu^{HLBL;\pi^0} = 5.76(38) \cdot 10^{-10}$ using Eqs. (15) and (16) respectively.

The nice agreement between all the different determinations of $a_\mu^{HLBL;PS}$ collected in Table III are quite reassuring. We should take the result using the $P_1^0(Q_1^2, Q_2^2)$ as our main result and the others as a reassessment of that one. On top we should add a 5% of systematic error yielding our final number as:

$$a_\mu^{HLBL;PS} = 8.9(6)(4) \times 10^{-10}. \quad (17)$$

in nice agreement with most of the recent phenomenological calculations for such quantity [70], but smaller than those determinations that model an off-shell TFF [67, 68, 77, 78], pointing toward a positive impact of the off-shellness of the pseudoscalar in such computation. Ref. [8] found, however, opposite conclusions, with a negative impact of the off-shellness of the pseudoscalars within the nonlocal quark model.

Ref. [70] provides with a compilation of the different contributions to the HLBL. They report a final value $a_\mu^{HLBL} = (10.5 \pm 2.6) \cdot 10^{-10}$. Updating the pseudoscalar piece of the HLBL considered in Ref. [70] using Eq. (17) and including all the other contributions collected there, we obtain $a_\mu^{HLBL} = (8.0 \pm 2.4) \cdot 10^{-10}$.

Primakoff determination of the two-photon partial decay width of the η meson are not included in the averaged fit on the Particle Data Tables [32]. If one would use that result (i.e., $\Gamma_{\eta \rightarrow \gamma\gamma} = 476(63)$ eV) instead, the result for the $a_\mu^{HLBL;\eta}$ would be reduced by a 7%. We remark, then, the need of a precise measurement for such partial decays in order to better constraint the impact of the TFF in the HLBL. We notice that such determination with precision of 1% would imply an error on HLBL of the same order.

V. CONCLUSIONS

In this article, we have analyzed the experimental data on the pseudoscalar Transition Form Factor at low and intermediate energies with a model-independent approach based on Padé Approximants. We extend the previous results for the π^0 -TFF [21] obtained with the Padé method to the η - and η' -TFF and we extracted their corresponding slopes and curvatures. The method used is simple and systematic and provides an estimation of the systematic errors.

The influence of our results for the η - and η' -TFFs on the $\eta - \eta'$ mixing is also analyzed. Finally, making use of the Padé technics and the large- N_c results for the hadronic light-by-light contribution to the $(g - 2)_\mu$ developed in Ref. [65], the impact of our results in this determination is also reported.

Acknowledgements

P.M would like to thank M. Vanderhaeghen, M. Unverzagt, C. Urbach and C.F. Redmer for discussions. Work supported by the Deutsche Forschungsgemeinschaft DFG through the Collaborative Research Center “The Low-Energy Frontier of the Standard Model” (SFB 1044), and partially by MICINN of Spain (FPA2010-16696), Junta de Andalucía (Grants No. P07-FQM 330 and No. P08-FQM 101).

Appendix A: Test of convergence of the PA sequence with a model

In this appendix we provide the parameterizations of our best $P_1^L(Q^2)$ fits for both the η - and η' -TFF. Defining $P_1^L(Q^2)$ as:

$$P_1^L(Q^2) = \frac{T_N(Q^2)}{R_1(Q^2)} = \frac{t_1 Q^2 + t_2 Q^4 + \dots + t_N (Q^2)^N}{1 + r_1 Q^2}, \quad (\text{A1})$$

the corresponding fitted coefficients⁴ for both η - and η' -TFF are collected in Table IV. $L = 5$ for the η case and $L = 6$ for the η' .

	η -TFF	η' -TFF
t_1	$0.274 Q^2$	$0.343 Q^2$
t_2	$0.098 Q^4$	$0.018 Q^4$
t_3	$0.682 \cdot 10^{-3} Q^6$	$0.255 \cdot 10^{-2} Q^6$
t_4	$0.184 \cdot 10^{-4} Q^8$	$0.182 \cdot 10^{-3} Q^8$
t_5	$0.105 \cdot 10^{-6} Q^{10}$	$0.585 \cdot 10^{-5} Q^{10}$
t_6		$0.664 \cdot 10^{-7} Q^{12}$
r_1	$1.950 Q^2$	$1.548 Q^2$

TABLE IV. Fitted coefficients for our best $P_1^L(Q^2)$ for the η - and η' -TFF.

Appendix B: Test of convergence of the PA sequence with a model

To test how fast the convergence of our PA sequence in the large- N_c limit (N_c been the number of colors) is, we

consider a Regge model for a pseudoscalar TFF (see, for example, [92–94] were similar large- N_c models are used to study the π^0 -TFF). In this limit, the vacuum sector of QCD becomes a theory of infinitely many non-interacting mesons and the propagators of the hadronic amplitudes are saturated by infinitely many sharp meson states. In the particular case below, the pion couples first to a pair of vector mesons V_ρ and V_ω which then transform into photons. Thus we have:

$$F_{P\gamma^*\gamma^*}(q_1^2, q_2^2) = \sum_{V_\rho, V_\omega} \frac{F_{V_\rho}(q_1^2) F_{V_\omega}(q_2^2) G_{PV_\rho V_\omega}(q_1^2, q_2^2)}{(q_1^2 - M_{V_\rho}^2)(q_2^2 - M_{V_\omega}^2)} + (q_1 \leftrightarrow q_2),$$

where F_{V_ρ} and F_{V_ω} are the current-vector meson couplings and $G_{PV_\rho V_\omega}$ is the coupling of two vector meson to the pseudoscalar π, η or η' . The dependence on the resonance excitation number n is the following

$$M_{V_\rho}^2 = M_{V_\omega}^2 = M^2 + n\Lambda^2, \text{ and } F_{V_\rho} = N_c V_\omega \equiv F. \quad (\text{B1})$$

The combination of sums in Eq. (B1) can be expressed in terms of the Digamma function $\psi(z) = \frac{d}{dz} \log \Gamma(z)$:

$$F_{P\gamma^*\gamma^*}(q_1^2, q_2^2) = F_{P\gamma^*\gamma^*}(Q^2, A) = \frac{c}{N_c A Q^2} \left[\psi \left(\frac{M^2}{\Lambda^2} + \frac{Q^2(1+A)}{2\Lambda^2} \right) - \psi \left(\frac{M^2}{\Lambda^2} + \frac{Q^2(1-A)}{2\Lambda^2} \right) \right], \quad (\text{B2})$$

where $Q^2 = -(q_1^2 + q_2^2)$, $A = \frac{q_1^2 - q_2^2}{q_1^2 + q_2^2}$ and c a constant [92, 93].

To reassemble the physical case we consider $N_c = 3$, $\Lambda^2 = 1.3 \text{ GeV}^2$ (as suggested by the recent light non-strange $q\bar{q}$ meson spectrum analysis [38] using the half-width rule [39]), $A = 1/2$, $M^2 = (0.8)^2 \text{ GeV}^2$ and the constant c in such a way that the anomaly $F_{P\gamma\gamma}(0,0) = \frac{1}{4\pi^2 f_P}$ is recovered.

Eqs. (B1) and (B2) use the large- N_c and chiral limits and thus have an analytic structure in the complex momentum plane which consists of an infinity of isolated

poles but no brunch-cut, i.e. they become meromorphic functions. As such, they have a well-defined series expansion in powers of momentum around the origin with a finite radius of convergence given by the first resonance mass. It is well-known [89] and largely explored in the context of Large- N_c [41, 42, 88] that the convergence of any near diagonal PA sequence to the original function for any finite momentum, over the whole complex plane (except perhaps in a zero-area set) is guaranteed.

By expanding Eq. (B2) one obtains the LEPs that are used to build up the $P_{N+1}^N(q_1^2, q_2^2)$ sequence. Each element of this sequence approximates better the low-energy region than the intermediate or large one, although as larger the sequence, larger the region well approximated. Comparing the $P_1^0(q_1^2, q_2^2)$, the $P_2^1(q_1^2, q_2^2)$ and so on with

⁴ For full precision of the coefficients together with the correlation matrix, contact the corresponding author.

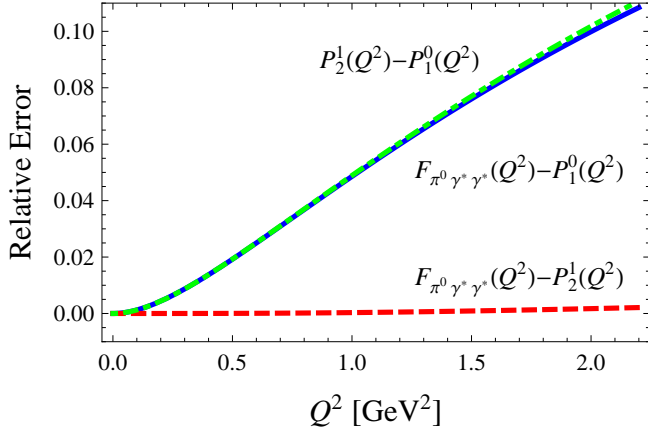


FIG. 5. Relative error for the first and second elements of the $P_{N+1}^N(Q^2)$ sequence compared to the TFF function Eq. (B2) (blue and red-dashed lines, resp.). The green-dotdashed line represents the relative error between the first and the second element on the approximant sequence.

$F_{P\gamma^*\gamma^*}(q_1^2, q_2^2)$ from Eq. (B2) one gets an idea of that q^2 -dependent systematic error. We show in Fig. 5 the relative error for both $P_1^0(q_1^2, q_2^2)$ and $P_2^1(q_1^2, q_2^2)$ compared to $F_{P\gamma^*\gamma^*}(q_1^2, q_2^2)$ (blue and red-dashed lines) but also the relative error between $P_1^0(q_1^2, q_2^2)$ and $P_2^1(q_1^2, q_2^2)$ (green-dotdashed line). We remark the similarity between the relative error of the $P_1^0(q_1^2, q_2^2)$ and the one between $P_1^0(q_1^2, q_2^2)$ and $P_2^1(q_1^2, q_2^2)$. This simple exercise suggests to use such difference to estimate the systematic error done with the $P_1^0(q_1^2, q_2^2)$.

In such a way, we define an error function $\epsilon(Q_1^2, Q_2^2)$ as such

$$F_{P\gamma^*\gamma^*}(Q_1^2, Q_2^2) = P_1^0(Q_1^2, Q_2^2)(1 + \epsilon(Q_1^2, Q_2^2)), \quad (\text{B3})$$

with $P_1^0(Q_1^2, Q_2^2)$ given in Eq. (13) and $\epsilon(Q_1^2, Q_2^2)$ emulating the difference between $P_1^0(q_1^2, q_2^2)$ and $P_2^1(q_1^2, q_2^2)$. As shown in Fig 5 the error increases with the energy reaching almost 10% of relative error for energies around 2 GeV, region which dominates the a_μ^{HLBL} . The error function can be naively parameterized as:

$$\epsilon(Q_1^2, Q_2^2) = \left(1 + \frac{Q_1^2}{20}\right) \left(1 + \frac{Q_2^2}{20}\right). \quad (\text{B4})$$

Computing the angular integrals accounting for a_μ^{HLBL} with Eq. (13) or Eq. (B3) yield a difference around 3% for the η case and around 5% for the η' (larger due to the larger normalization of the TFF). We suggested in the main text to ascribe a 5% of systematic error for both η and η' TFFs differences, which should account for any possible model-dependent extraction of such error.

Appendix C: Weighting functions

As demonstrated in [65], when a TFF parameterization can be cast in a generic form such as:

$$F_{P\gamma^*\gamma^*}(Q_1^2, Q_2^2) = -\frac{1}{4\pi^2 f_P} \left[f(-Q_1^2) + \sum_i \frac{1}{Q_2^2 + m_i^2} g_i(-Q_1^2) \right], \quad (\text{C1})$$

with m_i the poles of our approximants. Then, in the general two-loop expression for the pion-exchange contribution to the HLBL, the angular integrations can be performed using the hyperspherical approach. The HLBL piece can be then evaluated through the following expression:

$$a_\mu^{HLBL;PS} = \left(\frac{\alpha_{em}}{\pi}\right)^3 (a_{\mu(1)}^{PS} + a_{\mu(2)}^{PS}), \quad (\text{C2})$$

where

$$a_{\mu(1)}^{PS} = \int_0^\infty dQ_1 \int_0^\infty dQ_2 [\omega_1(Q_1^2, Q_2^2) G_1(Q_1^2, Q_2^2) + \omega_2(m_i, Q_1^2, Q_2^2) G_2(Q_1^2, Q_2^2)],$$

$$a_{\mu(2)}^{PS} = \int_0^\infty dQ_1 \int_0^\infty dQ_2 [\omega_3(m_i, Q_1^2, Q_2^2) G_3(Q_1^2, Q_2^2) + \omega_3(m_\pi, Q_1^2, Q_2^2) G_4(Q_1^2, Q_2^2)].$$

In the previous expressions, $\omega_i(Q_1^2, Q_2^2)$ are weight factors,

whose expressions are given in Ref.[65]. $G_i(Q_1^2, Q_2^2)$ are generalized form factors given by:

$$G_1(Q_1^2, Q_2^2) = \frac{f_P}{3} f(-Q_1^2) F_{P\gamma^*\gamma}(-Q_2^2, 0),$$

$$G_3(Q_1^2, Q_2^2) = \frac{f_P}{3} \frac{g(0)}{m_P^2 - m_i^2} F_{P\gamma^*\gamma}(-Q_1^2, -Q_2^2),$$

$$G_2(Q_1^2, Q_2^2) = \frac{f_P}{3} \frac{g(-Q_1^2)}{m_i^2} F_{P\gamma^*\gamma}(-Q_2^2, 0),$$

$$G_4(Q_1^2, Q_2^2) = \frac{f_P}{3} F_{P\gamma^*\gamma}(-Q_2^2, 0) \left(f(0) + \frac{g(0)}{m_P^2 - m_i^2} \right).$$

Notice that $G_1(Q_1^2, Q_2^2)$, $G_2(Q_1^2, Q_2^2)$ and $G_4(Q_1^2, Q_2^2)$ are built from the single-tagged TFF. With PA, the func-

tion $f(-Q^2) = 0$ in Eq. (C1) and $g(Q^2)$ is such to reproduce Eqs. (13) and (14).

-
- [1] B. Aubert *et al.* (BABAR Collaboration), Phys.Rev. **D80**, 052002 (2009), arXiv:0905.4778 [hep-ex].
- [2] J. Bijnens, A. Bramon, and F. Cornet, Phys.Rev.Lett. **61**, 1453 (1988).
- [3] J. Bijnens, A. Bramon, and F. Cornet, Z.Phys. **C46**, 599 (1990).
- [4] L. Ametller, J. Bijnens, A. Bramon, and F. Cornet, Phys.Rev. **D45**, 986 (1992).
- [5] S. J. Brodsky and G. P. Lepage, Phys.Rev. **D24**, 1808 (1981).
- [6] G. P. Lepage and S. J. Brodsky, Phys. Rev. **D22**, 2157 (1980).
- [7] P. Kroll, Eur.Phys.J. **C71**, 1623 (2011), arXiv:1012.3542 [hep-ph].
- [8] A. Dorokhov, A. Radzhabov, and A. Zhevlakov, Eur.Phys.J. **C71**, 1702 (2011), arXiv:1103.2042 [hep-ph].
- [9] S. J. Brodsky, F.-G. Cao, and G. F. de Teramond, Phys.Rev. **D84**, 033001 (2011), arXiv:1104.3364 [hep-ph].
- [10] C. Di Donato, G. Ricciardi, and I. Bigi, Phys.Rev. **D85**, 013016 (2012), arXiv:1105.3557 [hep-ph].
- [11] Y. N. Klopov, A. G. Oganesian, and O. V. Teryaev, Phys.Rev. **D84**, 051901 (2011), arXiv:1106.3855 [hep-ph].
- [12] X.-G. Wu and T. Huang, Phys.Rev. **D84**, 074011 (2011), arXiv:1106.4365 [hep-ph].
- [13] S. Noguera and S. Scopetta, Phys.Rev. **D85**, 054004 (2012), arXiv:1110.6402 [hep-ph].
- [14] I. Balakireva, W. Lucha, and D. Melikhov, Phys.Rev. **D85**, 036006 (2012), arXiv:1110.6904 [hep-ph].
- [15] H. Czyz, S. Ivashyn, A. Korchin, and O. Shekhovtsova, Phys.Rev. **D85**, 094010 (2012), arXiv:1202.1171 [hep-ph].
- [16] D. Melikhov and B. Stech, Phys.Rev. **D85**, 051901 (2012), arXiv:1202.4471 [hep-ph].
- [17] P. Kroll and K. Passek-Kumericki, J.Phys. **G40**, 075005 (2013), arXiv:1206.4870 [hep-ph].
- [18] D. Melikhov and B. Stech, Phys.Lett. **B718**, 488 (2012), arXiv:1206.5764 [hep-ph].
- [19] C.-Q. Geng and C.-C. Lih, Phys.Rev. **C86**, 038201 (2012), arXiv:1209.0174 [hep-ph].
- [20] Y. Klopov, A. Oganesian, and O. Teryaev, (2012), arXiv:1211.0874 [hep-ph].
- [21] P. Masjuan, Phys.Rev.D **86**, 094021 (2012), arXiv:1206.2549 [hep-ph].
- [22] P. Masjuan, S. Peris, and J. Sanz-Cillero, Phys.Rev. **D78**, 074028 (2008), arXiv:0807.4893 [hep-ph].
- [23] J. L. Rosner, Phys.Rev. **D79**, 097301 (2009), arXiv:0903.1796 [hep-ph].
- [24] D. Babusci, H. Czyz, F. Gonnella, S. Ivashyn, M. Mascolo, *et al.*, Eur.Phys.J. **C72**, 1917 (2012), arXiv:1109.2461 [hep-ph].
- [25] D. Asner, T. Barnes, J. Bian, I. Bigi, N. Brambilla, *et al.*, Int.J.Mod.Phys. **A24**, S1 (2009), arXiv:0809.1869 [hep-ex].
- [26] H. Czyz, A. Denig, M. De Stefanis, S. Eidelman, K. Griessinger, *et al.*, (2013), arXiv:1306.2045 [hep-ph].
- [27] G.A.Baker and P. Graves-Morris, *Pade Approximants*, edited by C. U. Press (Encyclopedia of Mathematics and its Applications, 1996).
- [28] H. J. Behrend *et al.* (CELLO), Z. Phys. **C49**, 401 (1991).
- [29] J. Gronberg *et al.* (CLEO), Phys. Rev. **D57**, 33 (1998), hep-ex/9707031.
- [30] P. del Amo Sanchez *et al.* (BABAR Collaboration), Phys.Rev. **D84**, 052001 (2011), arXiv:1101.1142 [hep-ex].
- [31] M. Acciarri *et al.* (L3 Collaboration), Phys.Lett. **B418**, 399 (1998).
- [32] J. Beringer *et al.* (Particle Data Group), Phys.Rev. **D86**, 010001 (2012).
- [33] A. Barabash *et al.* (KLOE-2 Collaboration), (2012), arXiv:1211.1845 [hep-ex].
- [34] B. Aubert *et al.* (BABAR Collaboration), Phys.Rev. **D74**, 012002 (2006), arXiv:hep-ex/0605018 [hep-ex].
- [35] H. Berghauer, V. Metag, A. Starostin, P. Aguar-Bartolome, L. Akasoy, *et al.*, Phys.Lett. **B701**, 562 (2011).
- [36] T. Pedlar *et al.* (CLEO Collaboration), Phys.Rev. **D79**, 111101 (2009), arXiv:0904.1394 [hep-ex].
- [37] L. Landsberg, Phys.Rept. **128**, 301 (1985).
- [38] P. Masjuan, E. R. Arriola, and W. Broniowski, Phys.Rev. **D85**, 094006 (2012), arXiv:1203.4782 [hep-ph].
- [39] P. Masjuan, E. Ruiz Arriola, and W. Broniowski, Phys.Rev. **D87**, 014005 (2013), arXiv:1210.0760 [hep-ph].
- [40] P. Masjuan, E. R. Arriola, and W. Broniowski, (2013), arXiv:1305.3493 [hep-ph].
- [41] P. Masjuan and S. Peris, JHEP **0705**, 040 (2007), arXiv:0704.1247 [hep-ph].
- [42] P. Masjuan and S. Peris, Phys.Lett. **B663**, 61 (2008), arXiv:0801.3558 [hep-ph].
- [43] P. Masjuan and J. Sanz-Cillero, (2013), arXiv:1306.6308 [hep-ph].
- [44] R. Dzhelezhyan, S. Golovkin, V. Kachanov, A. Konstanti-

- nov, V. Konstantinov, *et al.*, Phys.Lett. **B94**, 548 (1980).
- [45] R. Arnaldi *et al.* (NA60 Collaboration), Phys.Lett. **B677**, 260 (2009), arXiv:0902.2547 [hep-ph].
- [46] M. Hodana and P. Moskal (WASA-at-COSY Collaboration), (2012), arXiv:1210.3156 [nucl-ex].
- [47] R. Escribano, P. Masjuan, and P. Sánchez-Puertas, In preparation.
- [48] H. Leutwyler, Nucl.Phys.Proc.Suppl. **64**, 223 (1998), arXiv:hep-ph/9709408 [hep-ph].
- [49] A. Bramon, R. Escribano, and M. Scadron, Eur.Phys.J. **C7**, 271 (1999), arXiv:hep-ph/9711229 [hep-ph].
- [50] T. Feldmann, P. Kroll, and B. Stech, Phys.Rev. **D58**, 114006 (1998), arXiv:hep-ph/9802409 [hep-ph].
- [51] M. Benayoun, L. DelBuono, and H. B. O'Connell, Eur.Phys.J. **C17**, 593 (2000), arXiv:hep-ph/9905350 [hep-ph].
- [52] T. Feldmann, Int.J.Mod.Phys. **A15**, 159 (2000), arXiv:hep-ph/9907491 [hep-ph].
- [53] A. Bramon, R. Escribano, and M. Scadron, Phys.Lett. **B503**, 271 (2001), arXiv:hep-ph/0012049 [hep-ph].
- [54] N. Beisert and B. Borasoy, Eur.Phys.J. **A11**, 329 (2001), arXiv:hep-ph/0107175 [hep-ph].
- [55] J. Goity, A. Bernstein, and B. Holstein, Phys.Rev. **D66**, 076014 (2002), arXiv:hep-ph/0206007 [hep-ph].
- [56] R. Escribano and J.-M. Frere, JHEP **0506**, 029 (2005), arXiv:hep-ph/0501072 [hep-ph].
- [57] F. Ambrosino *et al.* (KLOE Collaboration), Phys.Lett. **B648**, 267 (2007), arXiv:hep-ex/0612029 [hep-ex].
- [58] R. Escribano and J. Nadal, JHEP **0705**, 006 (2007), arXiv:hep-ph/0703187 [hep-ph].
- [59] C. Thomas, JHEP **0710**, 026 (2007), arXiv:0705.1500 [hep-ph].
- [60] R. Escribano, P. Masjuan, and J. J. Sanz-Cillero, JHEP **1105**, 094 (2011), arXiv:1011.5884 [hep-ph].
- [61] J. Bijnens, E. Pallante, and J. Prades, Nucl.Phys. **B474**, 379 (1996), arXiv:hep-ph/9511388 [hep-ph].
- [62] M. Hayakawa, T. Kinoshita, and A. Sanda, Phys.Rev.Lett. **75**, 790 (1995), arXiv:hep-ph/9503463 [hep-ph].
- [63] J. Bijnens, E. Pallante, and J. Prades, Nucl.Phys. **B626**, 410 (2002), arXiv:hep-ph/0112255 [hep-ph].
- [64] M. Hayakawa and T. Kinoshita, Phys.Rev. **D57**, 465 (1998), arXiv:hep-ph/9708227 [hep-ph].
- [65] M. Knecht and A. Nyffeler, Phys.Rev. **D65**, 073034 (2002), arXiv:hep-ph/0111058 [hep-ph].
- [66] M. Knecht, A. Nyffeler, M. Perrottet, and E. de Rafael, Phys.Rev.Lett. **88**, 071802 (2002), arXiv:hep-ph/0111059 [hep-ph].
- [67] K. Melnikov and A. Vainshtein, Phys.Rev. **D70**, 113006 (2004), arXiv:hep-ph/0312226 [hep-ph].
- [68] A. E. Dorokhov and W. Broniowski, Phys.Rev. **D78**, 073011 (2008), arXiv:0805.0760 [hep-ph].
- [69] D. K. Hong and D. Kim, Phys.Lett. **B680**, 480 (2009), arXiv:0904.4042 [hep-ph].
- [70] J. Prades, E. de Rafael, and A. Vainshtein, (2009), arXiv:0901.0306 [hep-ph].
- [71] L. Cappiello, O. Cata, and G. D'Ambrosio, Phys.Rev. **D83**, 093006 (2011), arXiv:1009.1161 [hep-ph].
- [72] D. Greynat and E. de Rafael, JHEP **1207**, 020 (2012), arXiv:1204.3029 [hep-ph].
- [73] T. Goecke, C. S. Fischer, and R. Williams, (2012), arXiv:1210.1759 [hep-ph].
- [74] P. Masjuan and M. Vanderhaeghen, (2012), arXiv:1212.0357 [hep-ph].
- [75] J. Bijnens and M. Z. Abyaneh, EPJ Web Conf. **37**, 01007 (2012), arXiv:1208.3548 [hep-ph].
- [76] J. P. Miller, E. de Rafael, and B. L. Roberts, Rept.Prog.Phys. **70**, 795 (2007), arXiv:hep-ph/0703049 [hep-ph].
- [77] F. Jegerlehner and A. Nyffeler, Phys.Rept. **477**, 1 (2009), arXiv:0902.3360 [hep-ph].
- [78] A. Nyffeler, Phys.Rev. **D79**, 073012 (2009), arXiv:0901.1172 [hep-ph].
- [79] M. Davier, A. Hoecker, B. Malaescu, and Z. Zhang, Eur.Phys.J. **C71**, 1515 (2011), arXiv:1010.4180 [hep-ph].
- [80] K. Hagiwara, R. Liao, A. D. Martin, D. Nomura, and T. Teubner, J.Phys. **G38**, 085003 (2011).
- [81] G. Bennett *et al.* (Muon g-2 Collaboration), Phys.Rev.Lett. **92**, 161802 (2004), arXiv:hep-ex/0401008 [hep-ex].
- [82] G. Bennett *et al.* (Muon G-2 Collaboration), Phys.Rev. **D73**, 072003 (2006), arXiv:hep-ex/0602035 [hep-ex].
- [83] R. Carey, K. Lynch, J. Miller, B. Roberts, W. Morse, *et al.*, (2009).
- [84] G. 't Hooft, Nucl. Phys. **B72**, 461 (1974).
- [85] E. Witten, Nucl. Phys. **B160**, 57 (1979).
- [86] E. de Rafael, Phys.Lett. **B322**, 239 (1994), arXiv:hep-ph/9311316 [hep-ph].
- [87] S. Peris, M. Perrottet, and E. de Rafael, JHEP **9805**, 011 (1998), arXiv:hep-ph/9805442 [hep-ph].
- [88] P. Masjuan Queral, Ph.D. thesis, Universitat Autònoma de Barcelona (2010), arXiv:1005.5683 [hep-ph].
- [89] C. Pommerenke, J. Math. Anal. Appl. **41**, 775 (1973).
- [90] P. Masjuan and S. Peris, Phys.Lett. **B686**, 307 (2010), arXiv:0903.0294 [hep-ph].
- [91] E. Ruiz Arriola and W. Broniowski, Phys. Rev. **D81**, 054009 (2010), arXiv:1001.1636 [hep-ph] [hep-ph].
- [92] E. Ruiz Arriola and W. Broniowski, Phys. Rev. **D74**, 034008 (2006), arXiv:hep-ph/0605318.
- [93] E. Ruiz Arriola and W. Broniowski, Phys.Rev. **D81**, 094021 (2010), arXiv:1004.0837 [hep-ph].
- [94] K. Kampf and J. Novotny, Phys.Rev. **D84**, 014036 (2011), arXiv:1104.3137 [hep-ph].